# Design of a Dual-Band Three-Way Power Divider with Unequally High Power Split Ratio

*Minh Giang NGUYEN [1], Cong Tuan Nam NGUYEN [1], Tuan Hung NGUYEN [1], Hisashi MORISHITA [2]*

[1] Dept. of Radioelectronic Engineering, Le Quy Don Technical University, Hoang Quoc Viet Street 236, Hanoi, Vietnam
[2] Graduate School of Science and Engr., National Defense Academy, 1-10-20, Hashirimizu, Yokosuka, Kanagawa, Japan

hungnt1985_k31@lqdtu.edu.vn

Submitted February 4, 2023 / Accepted June 10, 2023 / Online first June 23, 2023

***Abstract.*** *In this paper, a dual-band three-way power divider with unequally high power split ratio is proposed. The dual-band operation is achieved by using a two-section impedance transformer, and to reach a high split ratio, transmission lines with impractical high characteristic impedances are replaced with dual-band T-shaped structures. The design is conducted with a thorough analysis and systematic design procedure for facilitating the rapid development of the prototypes. To verify the effectiveness of the proposed design method, an example of a power divider with a power split ratio of 7 : 5 : 1 is investigated, fabricated, and measured on a Rogers RO4003C substrate. Good agreements between the simulation and measurement results are obtained. Compared with several three-way unequal dual-band power dividers in previous works of the others, our proposed power divider delivered high power split ratio while still retaining good performances of insertion loss, return loss, and isolation between output ports.*

## Keywords

Wilkinson power divider, dual-band, high power split ratio, dual-band T-shaped structure, unequal division

## 1. Introduction

Power dividers are a key component that is widely used in many telecommunication subsystems, such as antenna feeding networks, mixers, and power amplifiers. Recently, there are increasing demands for PDs with the dual-band operation capability in relation to the multi-band microwave components. Various types of dual-band power dividers with equal [1–4] or unequal split ratios [5–7] have been proposed. Besides, many design methods for dual-band power dividers have been reported, such as using lumpled-elements [2], [8], two-section impedance transformer [9], open/shorted stubs [1], [2], and using T-configuration [10]. Although these prior PDs are good for an even number of output ports, it is still difficult to design unequal power dividers with an odd number of output ports. Especially, relatively few works have been focused on dual-band three-way power dividers with high power split ratio. In [11], a dual-band three-way power divider has been reported with a power split ratio of 3 : 1.5 : 1, showing that the maximum power split ratio only reached 3 : 1. The main problem in the design of a power divider with a large split ratio is it requires a branch with transmission lines of very large characteristic impedance, and the width of these transmission lines becomes too narrow to manufacture, while the limit values of the characteristic impedance of transmission lines are often less than 120 Ohms in general. On the other hand, in [12], a dual-band PD with a split ratio of 10 : 1 based on multi-T-section has been proposed, but this PD has only two output ports and has the disadvantage of relatively large dimensions.

In this paper, we combine the above techniques to propose a novel dual-band three-way Wilkinson power divider with a high power split ratio. To achieve dual-band operation, two-section impedance transformer [9] is employed. To reach a high power division ratio, impractical high-impedance lines in PD are replaced with dual-band T-shaped structures [12]. With this combination, the proposed PD exhibits high power split ratio and compact size simultaneously. The validity of the proposed method is confirmed by a design example in both simulation and measurement, and the comparison with the other designs.

## 2. Theory and Design Equations

### 2.1 Design a Three-Way Unequal Power Divider

The conventional three-way unequal PDs are composed of quarter-wavelength transmission lines with different impedances to match impedance between input and output ports as shown in Fig. 1 [13].

In Fig. 1, $Z_0$ dennotes source impedance and is equal to 50 Ω; $Z_1$, $Z_2$, and $Z_3$ are load impedances of output ports 2, 3, and 4 respectively. Resistors $R_{S1}$ and $R_{S2}$ are used to increase isolation performance between output ports.

DOI: 10.13164/re.2023.0338

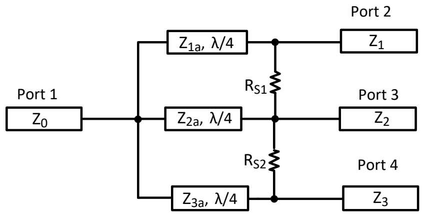


**Fig. 1.** The conventional three-way unequal power divider.

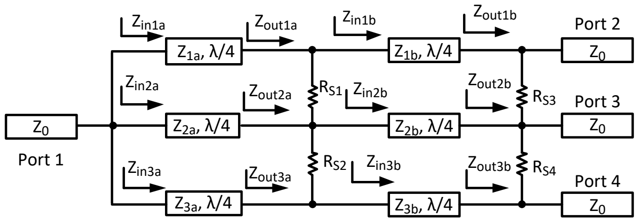


**Fig. 2.** The modified three-way unequal PD with output impedances of 50 ohms.

Assuming power split ratio is $P_2 : P_3 : P_4 = K_1^2 : K_2^2 : 1$, then the following equations are obtained [13]:

$$\frac{1}{Z_1}:\frac{1}{Z_2}:\frac{1}{Z_3}=K_1^2:K_2^2:1, \tag{1}$$

$$Z_{ja}=\frac{\sqrt{\left(1+K_1^2+K_2^2\right)Z_0Z_j}}{K_j}, \quad j=1,2,3. \tag{2}$$

From (1), the impedances $Z_1$, $Z_2$, and $Z_3$ can be determined as follows:

$$Z_1=\frac{aZ_0}{K_1^2},\ Z_2=\frac{aZ_0}{K_2^2},\ \ Z_3=aZ_0 \tag{3}$$

where $a$ is an arbitrary positive number. The value of $a$ needs to be appropriately selected so that the circuit can be fabricated in practice.

The PD in Fig. 1 has load impedances different from 50 Ω - standard impedance. So, this circuit is not convenient for use in practice. To overcome this shortcoming, we propose a modified PD (Fig. 2) of the PD in Fig. 1, in which quarter-wavelength transmission lines are employed to transform the values of $Z_1$, $Z_2$, and $Z_3$ to 50 Ω.

The values of $Z_{1b}$, $Z_{2b}$, and $Z_{3b}$ can be derived from the following:

$$Z_{jb}=\sqrt{50\cdot Z_j}\ ,\ j=1,2,3. \tag{4}$$

From the circuit in Fig. 2, the following equations can be obtained:

$$Z_{\text{in}ja}=\frac{\left(1+K_1^2+K_2^2\right)Z_0}{K_j^2},\ \ j=1,2,3, \tag{5}$$

$$Z_{\text{out1b}}=Z_{\text{out2b}}=Z_{\text{out3b}}=50\,\Omega, \tag{6}$$

$$Z_{\text{out}ja}=\frac{Z_{ja}^2}{Z_{\text{in}ja}},\quad j=1,2,3, \tag{7}$$

$$Z_{\text{in}jb}=\frac{Z_{jb}^2}{Z_{\text{out}jb}},\ \ j=1,2,3 \tag{8}$$

where $Z_{\text{in}ja}$ and $Z_{\text{out}ja}$ are input and output impedances of section $Z_{ja}$; $Z_{\text{in}jb}$ and $Z_{\text{out}jb}$ are input and output impedances of section $Z_{jb}$.

## 2.2 Design a Dual-band Three-Way Power Divider with Unequally High Power Split Ratio

To design a dual-band three-way PD, two-section impedance transformer [9] is applied to the scheme PD in Fig. 2. According to this method, the impedance $Z_{\text{in}}$ will be matched with impedance $Z_{\text{out}}$ at two arbitrary frequencies $f_1$ and $f_2$ ($f_1 < f_2$) using two transmission lines with characteristic impedances and electrical lengths $Z_{c1}$, $\theta$ and $Z_{c2}$, $\theta$ respectively (Fig. 3).

The values $Z_{c1}$, $Z_{c2}$ and $\theta$ can be determined as follows:

$$\beta=\frac{2\pi}{\lambda}, \tag{9}$$

$$L=\frac{\pi}{\beta_1+\beta_2}, \tag{10}$$

$$\alpha=\left(\tan\left(\beta_1 L\right)\right)^2, \tag{11}$$

$$Z_{c1}=\sqrt{\frac{Z_{\text{in}}\left(Z_{\text{out}}-Z_{\text{in}}\right)}{2\alpha}+\sqrt{\left[\frac{Z_{\text{in}}}{2\alpha}\left(Z_{\text{out}}-Z_{\text{in}}\right)\right]^2+Z_{\text{in}}^3 Z_{\text{out}}}}, \tag{12}$$

$$Z_{c2}=\frac{Z_{\text{in}}Z_{\text{out}}}{Z_{c1}}. \tag{13}$$

Applying two-section impedance transformer into the scheme in Fig. 2, each quarter-wavelength transmission line of the PD needs to be transformed into two sections with characteristic impedances and electrical lengths defined by (9)–(13). Thus, the proposed dual-band three-way PD is presented in Fig. 4.

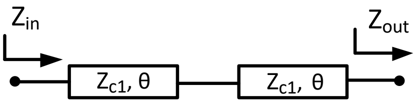


**Fig. 3.** Two-section dual-band transformer.

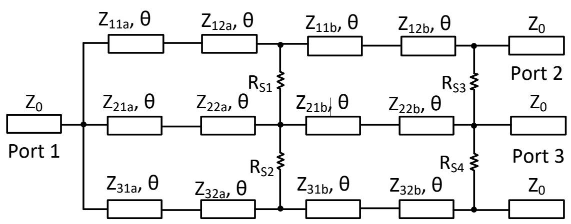


**Fig. 4.** The proposed dual-band three-way unequal power divider.

Resistors $R_{S1}$, $R_{S2}$, $R_{S3}$, and $R_{S4}$ are used to increase the isolation performance of the PD.

Assuming a power split ratio is $P_2 : P_3 : P_4 = K_1^2 : K_2^2 : 1$, then the output power at port 4 is the smallest compared with the other outputs. From (2)–(4) we get: $Z_{3a} = K_1^2 Z_{1a}$, $Z_{3a} = K_2^2 Z_{2a}$, $Z_{3a} = Z_{1b} K_1 \sqrt{1+K_1^2+K_2^2}$, $Z_{3a} = Z_{2b} K_2 \sqrt{1+K_1^2+K_2^2}$, $Z_{3a} = Z_{3b} \sqrt{1+K_1^2+K_2^2}$.

That is, $Z_{3a}$ is the largest impedance of the PD circuit presented in Fig. 2. After converting the circuit in Fig. 2 to the circuit in Fig. 4 using the two-section transformer technique, each transmission line is replaced with two segments. Transmission line with the largest characteristic impedance $Z_{3a}$ is converted into two transmission lines with characteristic impedances $Z_{31a}$ and $Z_{32a}$ and these impedances also become the greatest values of the circuit in Fig. 4.

To design a dual-band PD with a high power division ratio, we propose a new PD circuit, in which a dual-band T-shaped structure is used to replace transmission lines with the largest impedances $Z_{31a}$ and $Z_{32a}$. The structure of a dual-band T-section is presented in Fig. 5 [12].

The T-shaped structure consists of two transmission lines with impedance $Z_n$ and electrical length $\theta_n$ and one open stub with impedance $Z_m$ and electrical length $\theta_m$.

We need to define the design parameters of the T-section. Applying transmission line theory, the ABCD-matrix of a T-shaped structure is defined as follows:

$$\begin{bmatrix} A_1 & B_1 \\ C_1 & D_1 \end{bmatrix} = \begin{bmatrix} \cos(\theta_n) & \mathrm{i} Z_n \sin(\theta_n) \\ \dfrac{\mathrm{i}\sin(\theta_n)}{Z_n} & \cos(\theta_n) \end{bmatrix} \begin{bmatrix} 1 & 0 \\ \dfrac{\mathrm{i}\tan(\theta_m)}{Z_m} & 1 \end{bmatrix} \begin{bmatrix} \cos(\theta_n) & \mathrm{i} Z_n \sin(\theta_n) \\ \dfrac{\mathrm{i}\sin(\theta_n)}{Z_n} & \cos(\theta_n) \end{bmatrix}. \tag{14}$$

Meanwhile, the ABCD-matrix of a transmission line with high impedance $Z$ and electrical length $\theta$ is

$$\begin{bmatrix} A_2 & B_2 \\ C_2 & D_2 \end{bmatrix} = \begin{bmatrix} \cos(\theta) & \mathrm{i} Z \sin(\theta) \\ \dfrac{\mathrm{i}\sin(\theta)}{Z} & \cos(\theta) \end{bmatrix}. \tag{15}$$

By matching the ABCD parameters of a dual-band T-shaped structure with the transmission line with parameter $Z$ and $\theta$ we obtain the following equations:

$$Z_n = \frac{Z \cdot \cot(\theta_n)\sin(\theta)}{1+\cos(\theta)}, \tag{16}$$

$$Z_m = \frac{1}{2}\left[\frac{Z_n \cdot \tan(\theta_m)\sin(2\theta_n)}{\cos(2\theta_n)-\cos(\theta)}\right]. \tag{17}$$

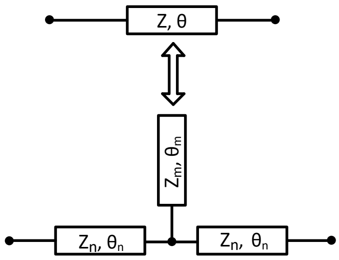


**Fig. 5.** Schematic diagram of a transmission line with a high impedance $Z$ and its equivalent dual-band T-shaped structure.

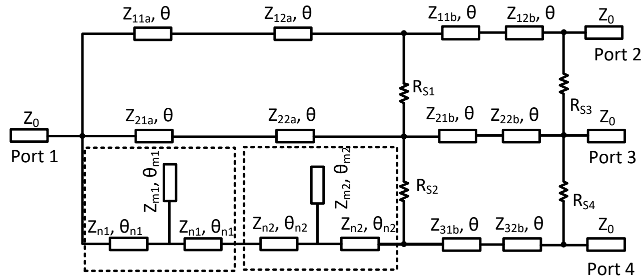


**Fig. 6.** The proposed dual-band three-way unequal PD with a high power split ratio.

To maintain dual-band operation of T-section and structural compactness, the following conditions must be satisfied:

$$\theta_n = \frac{\pi}{1+\dfrac{f_2}{f_1}}, \tag{18}$$

$$\theta_m = 2\theta_n \tag{19}$$

where $f_1$ and $f_2$ ($f_1 < f_2$) are designed operating frequencies.

Finally, the proposed two-band three-way power divider with a large split ratio has the form depicted in Fig. 6.

## 3. Simulations and Measurements

To validate the proposed design method, a dual-band three-way PD is designed for two frequencies of 1 GHz and 2 GHz with a high power split ratio $K_1 : K_2 : K_3 = 7 : 5 : 1$. The PD has been designed and fabricated on the Rogers RO4003C material with a thickness of 0.813 mm, a relative permittivity of 3.55, and a loss tangent of 0.0027.

Firstly, the coefficient $a$ in (3) needs to be defined. For this purpose, from (1)–(17) we plot the dependence of characteristic impedances of transmission lines in the PD against coefficient $a$ (Fig. 7). From the graphs in Fig. 7, we determined coefficient $a = 1.5$ to ensure all characteristic impedances are in the range of 15 Ω to 120 Ω.

It is found that, for a fixed power split ratio, the frequency ratio range between two operating frequencies is

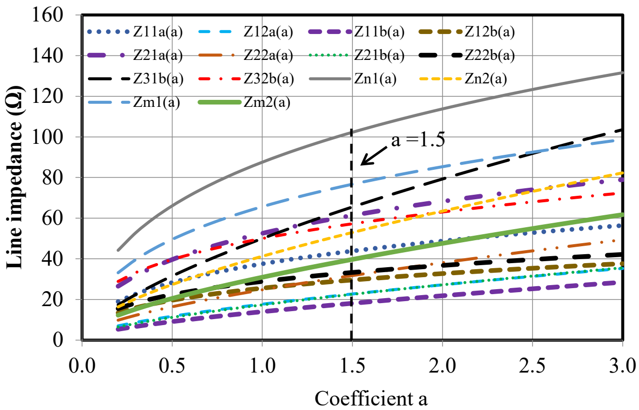


**Fig. 7.** Variation of characteristic impedances vs coefficient *a*.

| $a$ | $f_2/f_1$ |
|---|---|
| 2.3 | 1.63—2.12 |
| 2 | 1.65—2.14 |
| 1.5 | 1.71—2.19 |
| 1.3 | 1.73—2.22 |
| 1 | 2.24—2.26 |

**Tab. 1.** Variation of frequency ratio range versus coefficient *a* for power split ratio 7 : 5 : 1.

changed by varying the coefficient $a$. Table 1 shows the variation of the frequency ratio range versus coefficient $a$ with a power split ratio of 7 : 5 : 1. From Tab. 1, we can see that, when the coefficient $a$ is decreased, the values of the upper limit and the lower limit of the frequency ratio are increased. Therefore, the proposed circuit can be used to design dual-band PDs with arbitrary frequency ratio. In addition, the frequency ratio range can be changed by changing the coefficient $a$.

Next, we study the limitation of the power split ratio of the circuit to ensure that the circuit can be fabricated. The operating frequencies of the PD are fixed as 1 GHz and 2 GHz. Assuming a power split ratio is $P_2 : P_3 : P_4 = K_1^2 : K_2^2 : 1$ and $K_1 > K_2$. Then, the fabrication ability of the circuit depends on the value of $K_1$. Because $K_2$ does not affect the fabrication ability of the scheme, without losing generality, we assume that $K_2^2 = K_1^2/2$. Figure 8 shows the dependence of characteristic impedances of transmission lines in the PD against the value of $K_1^2$ (coefficient $a = 1.5$).

As can be seen from Fig. 8, to maintain all characteristic impedances in the range from 15 Ω to 120 Ω, the upper limit and the lower limit of the power split ratio $K_1^2$ is 10 and 3, respectively.

For fixed operating frequencies, by varying the coefficient $a$, the upper and lower limits of the power split ratio $K_1^2$ are changed. Table 2 shows the variation of the upper and lower limits of power split ratio $K_1^2$ versus coefficient $a$ with operating frequencies 1 GHz and 2 GHz.

Next step, the design parameters of the PD circuit in Fig. 2 are calculated: By using (3) the characteristic impedances are calculated as $Z_1 = 10.71$ Ω, $Z_2 = 15$ Ω, $Z_3 = 75$ Ω.

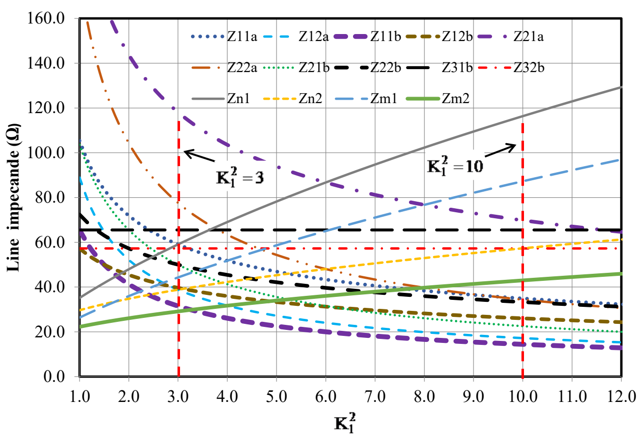


**Fig. 8.** Variation of characteristic impedances versus power split ratio $K_1^2$.

| $a$ | $K_1^2$ |
|---|---|
| 0.5 | 2—4 |
| 1 | 2.5—6 |
| 1.5 | 3—10 |
| 2 | 3.5—9 |

**Tab. 2.** Variation of the upper and the lower limits of the power split ratio $K_1^2$ versus coefficient *a* for operating frequencies 1 GHz and 2 GHz.

From (4), we have $Z_{1b} = 23.15$ Ω, $Z_{2b} = 27.39$ Ω, $Z_{3b} = 61.24$ Ω. Using (2), line impedances are computed as $Z_{1a} = 31.54$ Ω, $Z_{2a} = 44.16$ Ω, $Z_{3a} = 220.78$ Ω. Next, characteristic impedances of dual-band PD in Fig. 4 are defined: from (10), the electrical length of each transmission line is $\theta = 60°$. By using (5)–(13) line impedances on three branches of the circuit are computed:

Branch 1: $Z_{11a} = 43.84$ Ω, $Z_{12a} = 22.7$ Ω, $Z_{11b} = 18.11$ Ω, $Z_{12b} = 29.59$ Ω,

Branch 2: $Z_{21a} = 61.37$ Ω, $Z_{22a} = 31.77$ Ω, $Z_{21b} = 22.53$ Ω, $Z_{22b} = 33.29$ Ω.

Branch 3: $Z_{31a} = 306.86$ Ω, $Z_{32a} = 158.87$ Ω, $Z_{31b} = 65.51$ Ω, $Z_{32b} = 57.25$ Ω.

As we can see, $Z_{31a}$ and $Z_{32a}$ have impractical high impedances of 306.86 Ω and 158.87 Ω. These transmission lines have a width of 0.000173 mm and 0.067 mm, respectively, and they are unable to manufacture by normal PCB technology. Therefore, in the next step, transmission lines $Z_{31a}$ and $Z_{32a}$ are replaced with T-shaped structures. Using (14)–(17) the designed parameters of the T-shaped structure corresponding to $Z_{31a}$ are $\theta_{n1} = 60°$, $\theta_{m1} = 120°$, $Z_{n1} = 102.29$ Ω, $Z_{m1} = 76.71$ Ω. Similarly, for $Z_{32a}$ the calculated parameters as $\theta_{n2} = 60°$, $\theta_{m2} = 120°$, $Z_{n2} = 52.96$ Ω, $Z_{m2} = 39.72$ Ω. To achieve good isolation, the optimum parameters of resistors $R_{S1}$, $R_{S2}$, $R_{S3}$, and $R_{S4}$ are selected as follows: $R_{S1} = 30$ Ω, $R_{S2} = 68$ Ω, $R_{S3} = 300$ Ω, $R_{S4} = 1$ kΩ.

To demonstrate the effectiveness of the design approach, all characteristic impedance values of dual-band three-way PDs designed by the conventional method [9] and the proposed method are tabulated in Tab. 3.

| Conventional method [9] | | Proposed method | |
|---|---|---|---|
| **Impedance** | **Value (Ω)** | **Impedance** | **Value (Ω)** |
| $Z_{11a}$ | 43.84 | $Z_{11a}$ | 43.84 |
| $Z_{12a}$ | 22.7 | $Z_{12a}$ | 22.7 |
| $Z_{11b}$ | 18.11 | $Z_{11b}$ | 18.11 |
| $Z_{12b}$ | 29.59 | $Z_{12b}$ | 29.59 |
| $Z_{21a}$ | 61.37 | $Z_{21a}$ | 61.37 |
| $Z_{22a}$ | 31.77 | $Z_{22a}$ | 31.77 |
| $Z_{21b}$ | 22.53 | $Z_{21b}$ | 22.53 |
| $Z_{22b}$ | 33.29 | $Z_{22b}$ | 33.29 |
| $Z_{31a}$ | **306.86** | $Z_{n1}$ | **102.29** |
| $Z_{32a}$ | **158.87** | $Z_{m1}$ | 76.71 |
| $Z_{31b}$ | 65.51 | $Z_{n2}$ | 52.96 |
| $Z_{32b}$ | 57.25 | $Z_{m2}$ | 39.72 |
| | | $Z_{31b}$ | 65.51 |
| | | $Z_{32b}$ | 57.25 |

**Tab. 3.** Characteristic impedance values of the PD designed by the conventional method and the proposed method.

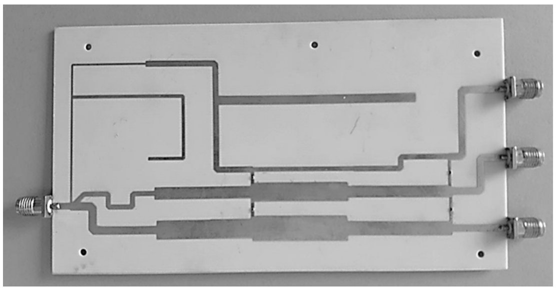

**Fig. 9.** Photograph of the fabricated dual-band three-way power divider with a power split ratio of 7 : 5 : 1.

From Tab. 3, it can be seen that the maximum characteristic impedance of transmission lines in the proposed scheme (Fig. 6) is 102.29 Ω. This means the minimum width of transmission lines is 0.39 mm. Therefore, the proposed PD is easy to be fabricated by normal PCB technology.

Figure 9 shows the fabricated prototype of the proposed PD. The total area of the PD is 132.5 mm × 75.1 mm.

The design program ADS 2019 is employed to make simulations and a Vector Network Analyzer PNA-X N5242A from Keysight is used to measure the performances of the fabricated PD (Fig. 10).

The simulated and measured insertion losses and input return loss S11 of the PD are shown in Fig. 11. As we can see, simulated results agree well with the measured ones. The measured center frequencies are found to be 0.98 GHz and 1.98 GHz, which are very close to the design frequencies 1 GHz and 2 GHz. The slight offset between design and measured results is due to tolerance in manufacturing.

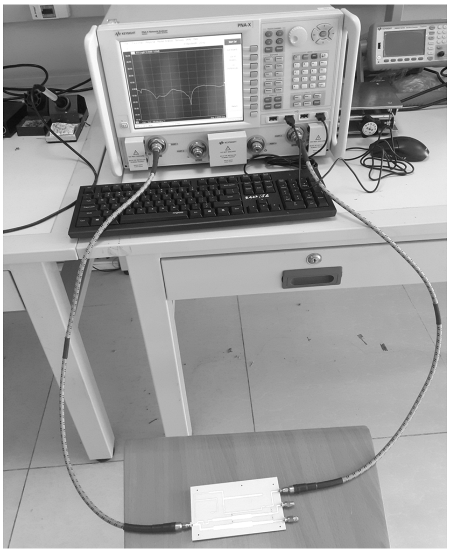

**Fig. 10.** Experimental setup.

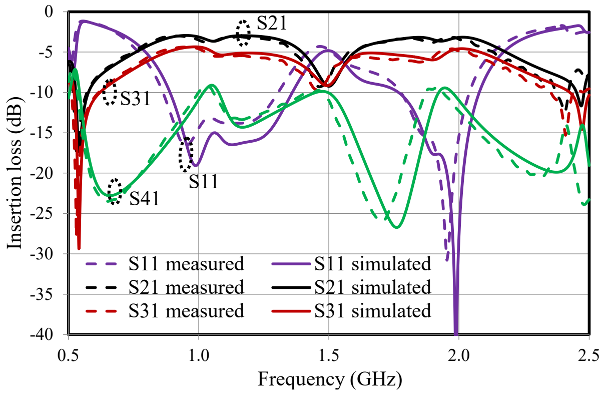


**Fig. 11.** Simulation and measurement results of insertion loss and input return loss of the proposed power divider.

From graphs in Fig. 11, the insertion loss at two central frequencies are: S21 = –3.29 dB, S31 = –4.47 dB, S41 = –10.96 dB at –0.98 GHz and S21 = –3.18 dB, S31 = –4.26 dB, S41 = –11.58 dB at 1.98 GHz (–2.69 dB, –4.15 dB, and –11.14 dB are the theoretical values for a 7 : 5 : 1 power divider). The measured input return loss at 0.98 GHz and 1.98 GHz are –15.62 dB and –20.3 dB, respectively.

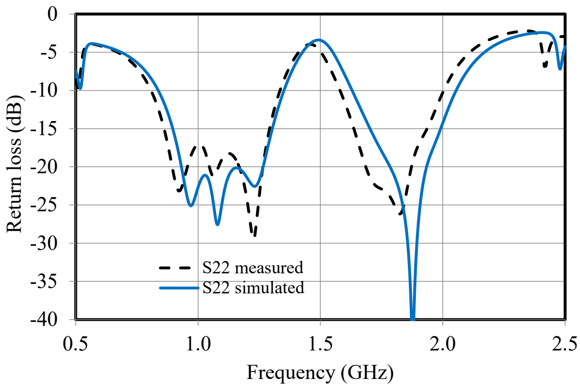


**Fig. 12.** Simulation and measurement of return loss S22 of the proposed power divider.

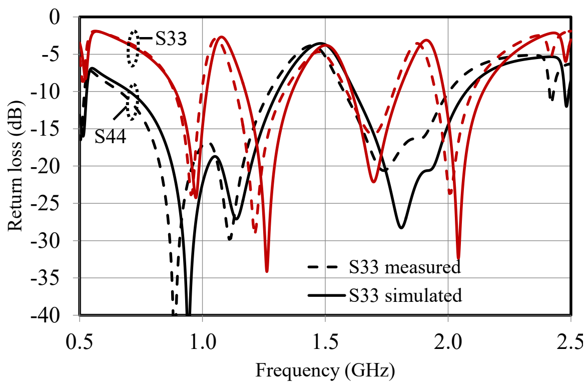


**Fig. 13.** Simulation and measurement of return losses S33 and S44 of the proposed power divider.

The simulated and measured output return losses of the designed PD are presented in Fig. 12, and 13. It is clear that the measured results are highly consistent with the simulated ones. Output return losses are better than –11 dB at two central frequencies.

Figures 14 and 15 show the simulation and measured isolation level between output ports of the designed PD. As can be seen from them, the measured isolation levels show good agreement with the simulation results. The measured isolation performances are better than –14.8 dB over two operating frequencies. Overall, the measured scattering parameters of the designed PD are tabulated in Tab. 4.

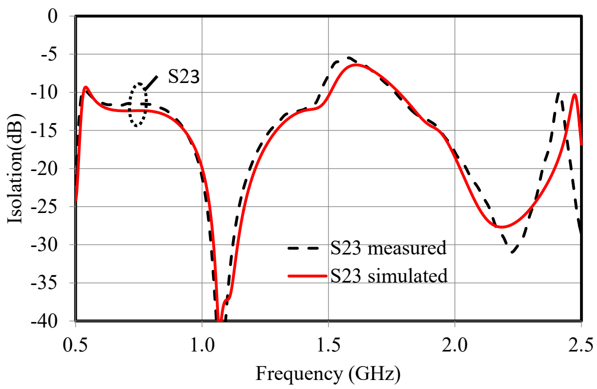


**Fig. 14.** Simulation and measurement parameter S23 of the proposed PD.

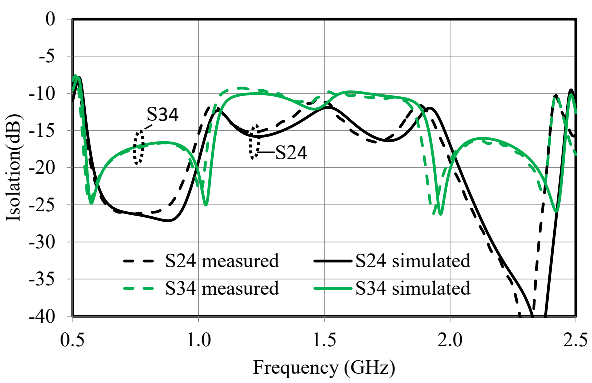


**Fig. 15.** Simulation and measurement of parameters S24 and S34 of the proposed PD.

| | 980 MHz | | 1980 MHz |
|---|---|---|---|
| S21 (dB) | –3.29 | –2.69 (ideal) | –3.18 |
| S31 (dB) | –4.466 | –4.15 (ideal) | –4.62 |
| S41 (dB) | –10.96 | –11.14 (ideal) | –11.58 |
| S11 (dB) | –15.62 | | –20.3 |
| S22 (dB) | –17.87 | | –11.75 |
| S33 (dB) | –18.28 | | –11.23 |
| S44 (dB) | –14.81 | | –16.74 |
| S23 (dB) | –18.58 | | –16.71 |
| S34 (dB) | –20.26 | | –20.23 |
| S24 (dB) | –17.71 | | –17.43 |

**Tab. 4.** Measured scattering parameters of the fabricated PD.

| | **This work** | **[14]** | **[15]** | **[16]** | **[17]** |
|---|---|---|---|---|---|
| ***f*** **(GHz)** | 0.98/1.98 | 0.9/1.4 | 1/4 | 2.43/5.06 | 0.9/2.1 |
| ***K*** | 7 : 5 : 1 | 1 : 4 : 1:<br>2 : 8 : 2 | 2 : 1 | 1 : 1 | 2 : 1 |
| ***N*** | 3 | 6 | 2 | 2 | 2 |
| **Δ (dB)** | > –0.6 | > –0.81 | > –0.9 | > –1.4 | > –0.6 |
| **IS (dB)** | < –16.7 | < –5.33 | < –18 | < –19.8 | < –26 |
| **RL (dB)** | < –11.23 | < –7.05 | < –15 | < –14.3 | NI |

**Tab. 5.** Comparisons of the proposed PD with other PDs.

To evaluate the effectiveness of the design approach, the measured performances of the proposed dual-band three-way PD compared with other reported works are summarized in Tab. 5.

In Tab. 5, we denote that Δ – The largest difference from ideal values of insertion loss; IS – Isolation; *N*– Number of output ports; *K* – Power split ratio; RL – Return loss, NI – No information.

Compared with other unequal and equal dual-band power dividers, we can see that the proposed power divider delivers a high power split ratio and low insertion loss. Other parameters, such as return loss and isolation between output ports are in good maintenance.

## 4. Conclusions

In this paper, a novel design approach of a dual-band Wilkinson PD with a high power split ratio is proposed. By replacing impractical high transmission lines with dual-band T-shaped sections, the proposed PD can achieve a high split ratio. To validate the proposed approach, a dual-band PD with a power split ratio of 7 : 5 : 1 was designed, fabricated, and tested. The simulated and measured results are in good agreement. Compared with the results of earlier works, the proposed PD exhibited a high split ratio, while still retaining good insertion loss, isolation, and return loss.

# References


[1] NATARAJAMANI, S., NAIR, R. G. Design theory of equal split dual-band power divider without reactive elements. *Advanced Electromagnetics*, 2022, vol 11, no 3, p. 78–83. DOI: 10.7716/aem.v11i3.1811

[2] PAKASIRI, C., WANG, S. Dual-band compact Wilkinson power divider using common inductor and complex load. *IEEE Access*, 2020, vol. 8, p. 97189–97195. DOI: 10.1109/ACCESS.2020.2995405

[3] XI, L., LIN, Y. A novel design of dual-band Wilkinson power divider with simple structure and wide band-ratios characteristics. *Journal of Electromagnetic Waves and Applications*, 2014, vol. 28, no. 13, p. 1635–1641. DOI: 10.1080/09205071.2014.938171

[4] WU, L., SUN, Z., YILMAZ, H., et al. A dual-frequency Wilkinson power divider. *IEEE Transactions on Microwave Theory and Techniques*, 2006, vol. 54, no. 1, p. 278–284. DOI: 10.1109/TMTT.2005.860300

[5] LI, B., WU, X., YANG, N., et al. Dual-band equal/unequal Wilkinson power dividers based on coupled-line section with short-circuited stub. *Progress In Electromagnetics Research*, 2011, vol. 111, p. 163–178. DOI: 10.2528/PIER10110108

[6] AHN, S.-H., LEE, J. W., CHO, C. S., et al. A dual-band unequal Wilkinson power divider with arbitrary frequency ratios. *IEEE Microwave and Wireless Components Letters,* 2009, vol. 19, no. 12, p. 783–785. DOI: 10.1109/lmwc.2009.2033503

[7] CHIU, L., XUE, Q. A parallel-strip ring power divider with high isolation and arbitrary power-dividing ratio. *IEEE Transactions on Microwave Theory and Techniques*, 2007, vol. 55, no. 11, p. 2419–2426. DOI: 10.1109/tmtt.2007.908669

[8] WANG, X., SAKAGAMI, I. Generalized dual-frequency Wilkinson power dividers with a series/parallel RLC circuit. In *2011 IEEE MTT-S International Microwave Symposium.* Baltimore (MD, USA), 2011, p. 1–4. DOI: 10.1109/MWSYM.2011.5972671

[9] MONZON, C. A small dual-frequency transformer in two sections. *IEEE Transactions on Microwave Theory and Techniques,* 2003, vol. 51, no. 4, p. 1157–1161. DOI: 10.1109/TMTT.2003.809675

[10] WU, Y., LIU, Y., ZHANG, Y., et al. A dual-band unequal Wilkinson power divider without reactive components. *IEEE Transactions on Microwave Theory and Technique*, 2009, vol. 57, no. 1, p. 216–222. DOI: 10.1109/TMTT.2008.2008981

[11] LI, Q., GONG, J.-G., LI, C.-L., et al. A compact dual-frequency three-way unequal power divider. *Journal of Electromagnetic Waves and Applications*, 2010, vol. 24, no. 2-3, p. 383–390. DOI: 10.1163/156939310790735714

[12] AL SHAMAILEH, K., DIB, N., ABUSHAMLEH, S. A dual-band 1:10 Wilkinson power divider based on multi-T-section characterization of high-impedance transmission lines. *IEEE Microwave and Wireless Components Letters*, 2017, vol. 27, no. 10, p. 897–899. DOI: 10.1109/LMWC.2017.2746665

[13] CHEN, H., ZHANG, T., CHE, W., et al. Compact unequal Wilkinson power divider with large power dividing ratio. In *2014 9th European Microwave Integrated Circuit Conference*. Rome (Italy), 2014, p. 608–611. DOI: 10.1109/EUMIC.2014.6997930

[14] KOURA, M. A., AL-ZAYED, A. S., CHEHIMI, M. M. Equal and unequal dual-band six-way power divider with band-distinct power division ratios. *Alexandria Engineering Journal*, 2023, vol. 66, p. 433–449. DOI: 10.1016/j.aej.2022.11.017

[15] WU, H., SUN, S., WU, Y., et al. Dual-band Gysel power dividers with large frequency ratio and unequal power division. *International Journal of RF and Microwave Computer-Aided Engineering,* 2020, vol. 30, no. 7. DOI: 10.1002/mmce.22203

[16] WANG, X., WANG, J., CHOI, W.-W., et al. Dual-wideband filtering power divider based on coupled stepped-impedance resonators. *IEEE Microwave and Wireless Components Letters*, 2018, vol. 28, no. 10, p. 873–875. DOI: 10.1109/LMWC.2018.2861578

[17] SHAO, C., XU, K., ZHU, X. H., et al. Dual-band filtering power divider with unequal power division ratio and low-loss characteristic. *International Journal of RF and Microwave Computer-Aided Engineering,* 2020, vol. 30, no. 5. DOI: 10.1002/mmce.22149


# About the Authors ...

**Minh Giang NGUYEN** was born in Thai Nguyen, Vietnam. He received a D.E. degree in Electronics Engineering from Irkutsk National State Technical University, Russia in 2018. He is currently a lecturer at the Le Quy Don Technical University, Hanoi, Vietnam. His research interests include RF design and microwave engineering.

**Cong Tuan Nam NGUYEN** was born in Phu Tho, Vietnam. He is studying at Le Quy Don Technical University, Hanoi, Vietnam. His research interests include RF design and microwave engineering.

**Tuan Hung NGUYEN (**corresponding author) was born in Nam Dinh, Vietnam, on August 2, 1985. He received the B.S., M.S., and Ph.D. degrees in the Department of Electrical and Electronic Engineering from the National Defense Academy of Japan in 2010, 2012, and 2015, respectively. He is currently a lecturer at the Faculty of Radio-Electronic Engineering, Le Quy Don Technical University, Vietnam. His research interests include the design of antennas and filters for mobile handset devices, communication and radar systems, multistatic radar systems, and signal processing for radar systems.

**Hisashi MORISHITA** received the B.S. degree in Electrical Engineering from the National Defense Academy of Japan in 1980, the M.S. and Ph.D. degrees from University of Tsukuba in 1987 and 1990, respectively. From 1990 to 1992, he worked as a research and development officer at the Air Research and Development Command of Japan Air Self-Defense Force (JASDF). Since 1992, he has been with the National Defense Academy and is currently a Professor in the Department of Electrical and Electronic Engineering. From 1996 to 1997, he was a Visiting Researcher at the Communications Research Laboratory, McMaster University, Canada. His research is concerned with mobile communication, small antennas, multistatic radar systems, and signal processing for radar systems. He is a senior member of IEEE.